



# Evaluation of the application of suspensions of iron oxide magnetic nanoparticles functionalized with quaternized chitosan and phosphates on yellow maize and chili pepper plants

A. A. Velásquez<sup>1</sup> · J. P. Urquijo<sup>2</sup> · Y. A. Montoya<sup>3</sup> · D. M. Susunaga<sup>3</sup> ·  
D. F. Villanueva-Mejía<sup>3</sup>

Accepted: 2 January 2024  
© The Author(s) 2024

## Abstract

We have applied aqueous suspensions of magnetite-maghemite nanoparticles functionalized with quaternized chitosan and phosphate groups on yellow maize (*Zea Mays*) and chili pepper (*Capsicum annuum*) plants, at greenhouse conditions, to evaluate if any beneficial or adverse effects are produced by these nanocomposites in the development of these kind of plants at morphological and physiological level. Phytotoxicity assays with yellow maize seeds showed excellent germination percentages in all treatments evaluated, as well as increasing indicators of biomass and root length of germinated seeds for suspensions of nanoparticles with iron contents up to 50 ppm. Suspensions of nanoparticles with iron contents higher than 50 ppm led to decreasing indicators of biomass and root length of germinated seeds compared to lower iron contents. Iron contents of 100 ppm showed indicators lower than those of the control, suggesting phytotoxic effect of these nanocomposites for iron contents above 100 ppm. Measurements of morphological and physiological parameters of plants of both crops in greenhouse conditions, treated with suspensions of nanoparticles with iron-phosphorus contents of 25–3, 35–4 and 45–5 ppm, commercial fertilizer as positive control and tap water as a negative control did not evidence any phytotoxic or beneficial effect. The results suggest that, although these nanocomposites did not have a noticeable effect as vehicles of micro and macro nutrients as iron and phosphorus in the evaluated plants, they did not produce phytotoxic effects on them at the morphological and physiological level for iron contents less than 50 ppm, as they showed adequate growth and development.

**Keywords** Magnetite-Maghemite · Nanocomposites · Maize and chili pepper · Phytotoxicity · Mössbauer spectroscopy

## 1 Introduction

The growing demand for food worldwide, due to the continuous increase in population, has caused an excessive use of agrochemicals and inadequate agricultural practices, resulting in low crop yields, negative health effects and negative environmental impacts. To counteract these negative consequences, innovative alternatives are being developed to build a sustainable agricultural model [1], among which are nanofertilizers, whose main objective is to provide micro and macronutrients to crops in an efficient and environmentally friendly way. However, the effect of these nanomaterials on plant growth and development is still unclear [2]. Several kinds of metal oxide nanoparticles (NPs), such as iron oxide NPs, have been applied in agriculture, specifically in plant protection and fertilization experiments [3–6]. Some of these studies have reported that iron oxide NPs can increase seed germination index [3, 7], seedling vigor, plant biomass, and yield and enhance physiological function [3, 8]. To achieve biocompatibility, biodegradation, and stability of the NPs, as well as to modulate any toxic or agglomerative effect in physiological environments, their surface can be coated with polymeric materials for obtaining core-shell type structures (nanocomposites) whose chemical structure can be modified to improve their solubility at physiological pHs [9, 10]. Chitosan, an amino polysaccharide, is obtained from the deacetylation of chitin, a polysaccharide present mainly in the exoskeletons of crustaceans. Chitosan has desirable properties in biotechnological applications since it is biocompatible, biodegradable, and has antifungal and antimicrobial activity, however, due to its low solubility at physiological pHs, its use in biological systems is limited. This drawback can be overcome by chemically modifying the chitosan structure, such as binding for quaternary ammonium groups [11]. On the other hand, to our knowledge, there are not enough studies that examine the impact of iron oxide nanoparticles coated with chitosan on maize plants (*Zea mays*), a crop of great importance for the food security of humankind, the majority of the published nanotoxicology articles have focused on mammalian cytotoxicity or impacts in animals and bacteria. Only a few studies have considered the toxicity of NPs in plant systems [12]. To contribute to elucidating the effect of iron oxide nanocomposites on cereal crops, we evaluated the effect of the application of suspensions of magnetite-maghemite NPs, functionalized with quaternized chitosan and phosphates, as phosphorus source, on the morphological parameters of yellow maize plants (variety FNC31AC). Details of the experiments and results obtained are presented in the following sections of this paper.

## 2 Materials and methods

### 2.1 Materials

For the synthesis of the nanocomposites, the following reagents were used: Chitosan (degree of deacetylation > 75%), Glycidyl trimethylammonium chloride (GTMAC), Perchloric acid  $\text{HClO}_4$  (70–72%),  $\text{FeCl}_3 \cdot 6\text{H}_2\text{O}$ ,  $\text{Fe}(\text{NH}_4)_2(\text{SO}_4)_2 \cdot 6\text{H}_2\text{O}$ , Sodium hydroxide NaOH and oxalic acid  $\text{C}_2\text{H}_2\text{O}_4$ . All reagents, with the exception of phosphate precursor, were of analytical grade, and they were used as received. Phosphate rock was obtained in a Colombian mine, this is due to this research intends to obtain the macronutrient for the plants from an abundant resource of this product in Colombia, in this case, a mine, seeking to contribute to

development of sustainable agriculture, however, we would expect that an analytical grade phosphate precursor could be used in this experiment without significant variation in results.

## 2.2 Preparation of N-2-hydroxy-propyl-3-trimethyl ammonium chitosan chloride (HTCC)

Quaternization of chitosan is a process necessary to increase the solubility of this polymer in the alkaline conditions required to obtain magnetite-maghemite for co-precipitation. HTCC was synthesized by a reaction with GTMAC at 80 °C employing the method of Ruihua et al. [11] with some modifications. For this purpose, 1 g of chitosan was suspended in 150.0 mL of deionized water at 60 °C and dissolved by the addition of 1.0 mL of HClO<sub>4</sub> under stirring. Afterward 8.0 mL of GTMAC was added in two portions at intervals of 0.5 h. Subsequently, the reaction continued at 80 °C for 8 h. The HTCC obtained was precipitated of the reaction solution with acetone and it was dried and resuspended in deionized water for their posterior use.

## 2.3 Preparation of aqueous suspensions of magnetic nanocomposites coated with quaternized chitosan

Magnetite-maghemite nanoparticles functionalized with quaternized chitosan (Fe<sub>3</sub>O<sub>4</sub>-QC) were prepared by chemical coprecipitation of Fe<sup>3+</sup> and Fe<sup>2+</sup> species in presence of a quaternized chitosan solution. As a first step, 0.500 g of quaternized chitosan were dissolved in 100.0 mL of deionized water, and the solution was bubbled with N<sub>2(g)</sub> for 30 min. Afterwards the pH of the solution was increased to 10 with the controlled addition of a solution 1 M NaOH. Subsequently, a solution containing 0.500 g of Fe(NH<sub>4</sub>)<sub>2</sub>(SO<sub>4</sub>)<sub>2</sub>·6H<sub>2</sub>O and 0.700 g of FeCl<sub>3</sub>·6H<sub>2</sub>O was added, and a black suspension was obtained. The suspension obtained was left under stirring for one hour and subsequently washed by dialysis.

## 2.4 Binding of PO<sub>4</sub><sup>3-</sup> ions to the surface of Fe<sub>3</sub>O<sub>4</sub>-QC

For obtaining the PO<sub>4</sub><sup>3-</sup> ions to be bonded to the Fe<sub>3</sub>O<sub>4</sub>-QC surface, 2 g of phosphoric rock were dissolved in 100 mL of a 2% solution in oxalic acid. The mixture was heated for 4 h at 80 °C, then allowed to stand for 24 h and filtered. Afterward, 50 mL of this solution were mixed with 100 mL of the Fe<sub>3</sub>O<sub>4</sub>-QC suspension and stirred for 1 h. The suspension obtained was washed by dialysis, and the concentrations of phosphates and iron in the solution were determined by spectrophotometric measurements.

## 2.5 Characterization of magnetic nanocomposites

The synthesized nanocomposites were characterized by structural, chemical and magnetic techniques. X-ray measurements were taken with a PANalytical X'Pert PRO diffractometer, with Cu-K<sub>α</sub> radiation ( $\lambda=1.540598 \text{ \AA}$ ), angular range  $2\theta$ : 15°-80°, step of 0.05° and counting time of 1 s per step. Fourier transform infrared spectroscopy (FTIR) measurements were obtained with a Perkin Elmer infrared spectrometer, model Spectrum Two. Room temperature transmission Mössbauer measurements were taken with a Mössbauer spectrometer developed at the Laboratory of Instrumentation and Spectroscopy of the University EAFIT

[13], which operates in the constant acceleration mode, with a radioactive source of  $^{57}\text{Co}/\text{Rh}$  with initial activity of 25 mCi and speeds between  $-12$  and  $12 \text{ mm s}^{-1}$ . Mössbauer absorbers were prepared by diluting the sample in sugar until an effective thickness of  $6 \text{ mg-Fe cm}^{-2}$  was obtained. Magnetization curves were taken with a vibrating sample magnetometer developed at the Instrumentation and Spectroscopy Laboratory of the EAFIT University, with a resolution of  $3 \times 10^{-7} \text{ A m}^2$  in magnetic moment and a range of  $438 \text{ kA m}^{-1}$  in the magnetic field. The iron and phosphorus contents in the aqueous suspensions of MNPs were quantified by UV-Vis spectroscopy, with a spectrophotometer Thermo Scientific GENESYS 150 UV-Vis.

## 2.6 Seeds preparation

Seeds of yellow hybrid maize, reference FNC31AC, were supplied by “Federación Nacional de Cultivadores de Cereales, Leguminosas y Soya (FENALCE)” from Colombia. It is a quality protein maize (QPM), which means that these seeds can synthesize a high quantity of the essential amino acids of lysine and tryptophan, thanks to the fact that they contain the *opaco-2* gene. Its adaptation is optimal in the Colombian coffee zone, with altitudes between 1200 and 1800 m.a.s.l [14]. Chili pepper seeds were obtained from an agricultural supermarket (“Tierragro”) located in Medellín, Colombia, these belong to a species called *Capsicum annuum L.* which grows in tropical climates and has a potential as an antioxidant and anti-obesity agent, bioactive compounds important to reduce the risk of some non-communicable diseases, which gives this crop an important position in the world economy [15]. Maize seeds were subjected to a disinfection process before being used in the phytotoxicity assay. This disinfection process was previously standardized at the Plant Biotechnology laboratory at the EAFIT University, and it is included as supplementary material. Initially, seeds were rinsed with a solution of iodine, soap and water. Afterwards, the seeds were immersed in 15% sodium hypochlorite for 3 min and then rinsed three times with sterile deionized water. Finally, the seeds were left to dry in a laminar flow chamber for approximately 10 min. Maize and chili pepper seeds were not disinfected for greenhouse assay.

## 2.7 Phytotoxicity assay

Maize seeds were chosen as a study model for this assay, because we had already worked with it in previous projects, which allows us to have a better knowledge of this seed and thus to identify more easily the morpho-anatomical changes that occurred during this test, which evaluated the phytotoxicity effect of a broad spectrum of nanoparticle suspensions in order to define the most suitable concentrations for the greenhouse test described below. It consisted of placing 10 maize seeds per Petri dish (100 mm x 15 mm) with a cellulose filter paper at the bottom impregnated with 3 mL of deionized water (control) or with suspensions of nanoparticles with different iron contents (12.5, 25, 50, 75 and 100 ppm). Petri dishes were stored in a dark place at  $23 \text{ }^\circ\text{C}$  for 28 days. After this time, the seed germination percentage and root length of germinated seeds were recorded. Each treatment was carried out in triplicate.

**Table 1** Labels of the suspensions of nanoparticles used in the treatments according to their contents of iron and phosphorus

Suspension label	Iron content (ppm)	Phosphorus content (ppm)
25–3	25	2.86
35–4	35	4
45–5	45	5.15

## 2.8 Preparation of the aqueous suspensions of magnetic nanoparticles

To adjust the content of iron and phosphorus supplied by the suspension of nanoparticles used in greenhouse assay, the initial suspension of nanoparticles was diluted in tap water. Table 1 presents the labels used to distinguish the suspensions according to their iron and phosphorus contents. The maximum content of phosphorus bound to the surface of nanoparticles with the highest iron content (45 ppm) was 5.15 ppm.

## 2.9 Greenhouse assay

Based on the results of the phytotoxicity test, three suspensions of nanoparticles with iron contents below 50 ppm were selected to evaluate morphoanatomical and physiological parameters in maize and chili plants under greenhouse conditions. For this purpose, five maize seeds and three chili pepper seedlings were sown in two-layer bags with 10 kg of substrate, previously treated with lime, at an average temperature and humidity of 29 °C and 60%, respectively. Fifteen days after sowing, only one seedling was left in each of the bags, the one that had adapted best to the conditions of the trial. Thus, with only one plant per bag, there were a total of 65 seedlings for each of the crops, 13 replicates per treatment (25–3 ppm, 35–4 ppm and 45–5 ppm of the suspension of nanoparticles, a commercial fertilizer as a positive control and tap water as a negative control). The application of the treatments, in edaphic form, was initiated 15 days after sowing and it was repeated at four different times defined in each of the crop cycles. After four months, the plants were harvested and sent to EAFIT University to measure the following morpho-anatomical and physiological variables: plant height, fruit weight, stem thickness and dry biomass.

## 2.10 Statistical analysis

In the phytotoxicity assay, three replicates with 10 individuals per treatment of maize seeds were considered. The data were evaluated by regression analysis, in which the parameter values were considered to determine the relationship between the dependent variables (biomass, root length) with respect to the independent variable (iron contents). For the greenhouse assay, we evaluated 25–3, 35–4 and 45–5 ppm of iron and phosphorus content ( $n=13$  per treatment, per crop), data were analyzed using one-way analysis of variance ANOVA [16] to determine significant differences between treatments, followed by a Dunnett's tests for multiple comparisons at a 95% confidence level. Statistical analysis was performed with the Statgraphics software, version 19 and RStudio software version 4.2.2.

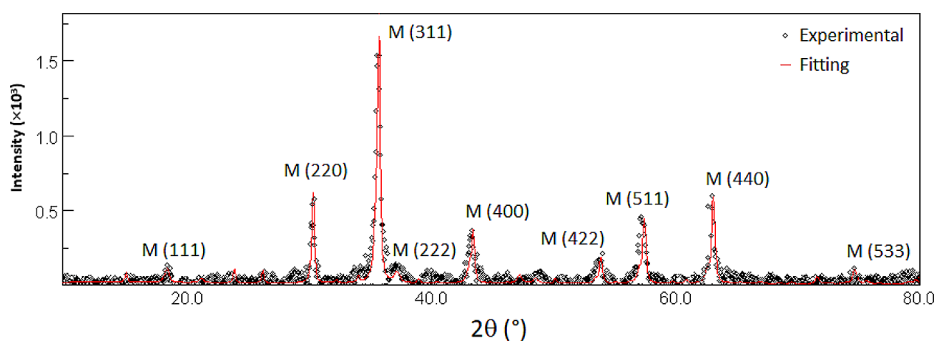


**Fig. 1** Diffractogram of the nanocomposite sample of magnetite-maghemite functionalized with chitosan and phosphate groups. Letter M stands for magnetite and maghemite

**Table 2** Structural parameters of the nanoparticles obtained by Rietveld refinement

Phase	$a$ (Å)	$D$ (nm)
Magnetite-Maghemite	$8.377 \pm 0.004$	$18 \pm 2$

$a$ : lattice parameter  $D$ : mean crystallite diameter

## 3 Results and discussion

### 3.1 Characterization of the nanoparticles

#### 3.1.1 X-ray measurements

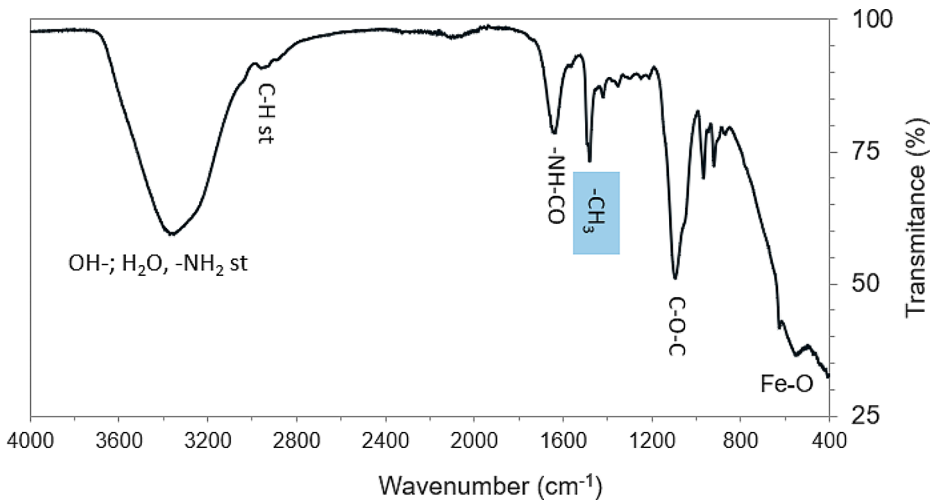
Figure 1 shows the X-ray diffractogram of the synthesized nanocomposite. The diffractogram was processed with the software Powder X [17] to remove the continuous background signal of the tube. We applied Rietveld refinement with the software MAUD (Material Analysis Using Diffraction) [18] to obtain lattice parameter ( $a$ ) and mean crystallite diameter of the sample ( $D$ ), which are presented in Table 2. Only peaks of magnetite and maghemite, labeled M, were identified in the diffractogram, which can be corroborated by the sequence of peaks indexed. Both phases were indistinguishable in the diffractogram because of their very similar structural parameters.

#### 3.1.2 FTIR measurements

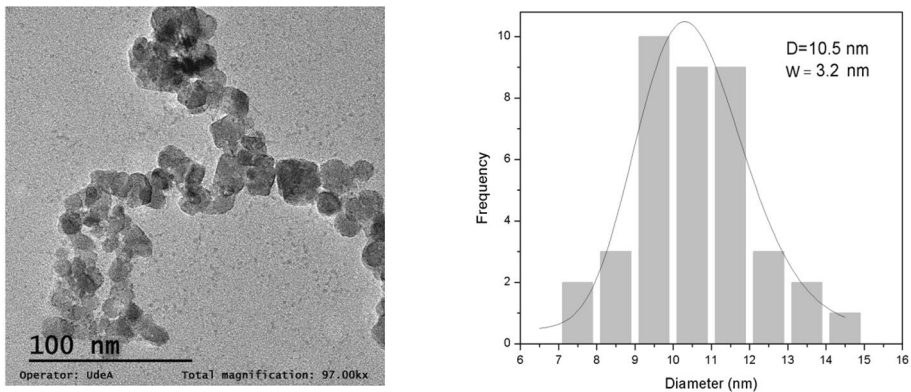
Figure 2 presents the infrared spectrum of the nanocomposites; this spectrum shows several bands characteristic of Fe-O bonds, as well as polysaccharide chains of chitosan, among them Ether (C-O-C), Amide (-NH-CO) and C-H. This spectrum also shows a band placed around  $1478 \text{ cm}^{-1}$ , characteristic of methyl group (-CH<sub>3</sub>). The presence of methyl group evidences the quaternization of the chitosan bonded to the surface of the spinel nanoparticles.

#### 3.1.3 TEM measurements

Figure 3a,b show the TEM micrograph of the nanoparticles obtained and their particle size distribution, respectively. As can be seen from the micrograph, the particles exhibited a



**Fig. 2** FTIR spectrum of the nanocomposite synthesized

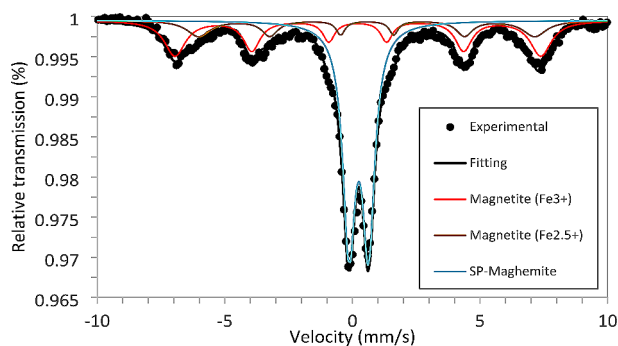


**Fig. 3** **a** TEM micrograph of the nanocomposite synthesized, **b** Particle size distribution histogram

quasi-spherical morphology, with a mean particle size around 11 nm, estimated by the log-normal fitting of the particle size distribution.

### 3.1.4 Mössbauer measurements

The room temperature Mössbauer spectrum of the nanoparticles is presented in Fig. 4, while Table 3 presents the hyperfine parameters derived from the fitting of the spectrum with Lorentzian profile lines, by using the least square software MOSF [19]. Data with the original spectrum, the fitted spectrum and the hyperfine parameters obtained by fitting are included in the section of supplementary material. The spectrum was well fitted with two sextets and one doublet. The sextet with hyperfine magnetic field of 44.1 T is attributed to an average contribution of ions  $\text{Fe}^{3+}$  of magnetic ordered magnetite and maghemite,

**Fig. 4** Mössbauer spectrum of the nanocomposite synthesized**Table 3** Hyperfine and spectral parameters of the iron phases identified in the nanoparticles

$B_{hf}$  hyperfine magnetic field,  $\delta$  isomer shift relative to  $\alpha$ -Fe,  $2\epsilon$  and  $\Delta E_Q$  quadrupole splitting for sextets and doublets, respectively,  $W$  line width of the innermost lines of each spectrum,  $A$  spectral area

Subspectrum	$B_{hf}$ (T)	$\delta$ (mm s <sup>-1</sup> )	$2\epsilon$ , $\Delta E_Q$ (mm s <sup>-1</sup> )	$W$ (mm s <sup>-1</sup> )	$A$ (%)
Magnetite-maghemite Fe <sup>3+</sup>	44.1 ± 0.2	0.32 ± 0.02	0.02 ± 0.02	0.60 ± 0.02	28 ± 2
Magnetite Fe <sup>2.5+</sup>	40.7 ± 0.2	0.62 ± 0.02	0.02 ± 0.02	0.77 ± 0.02	22 ± 2
SP-Maghemite Fe <sup>3+</sup>	---	0.35 ± 0.02	0.75 ± 0.02	0.63 ± 0.02	50 ± 2

this sextet may also have the contribution of core nanostructures of magnetite covered by a shell of maghemite. The sextet with hyperfine magnetic field of 40.7 T is attributed to ions Fe<sup>2.5+</sup> at octahedral sites of magnetite, where electronic hopping between Fe<sup>2+</sup> and Fe<sup>3+</sup> cations occupying neighboring octahedra takes place, being the intermediate valence 2.5+ confirmed by the isomer shift around 0.6 mm/s exhibited by the second sextet.

Although hyperfine magnetic fields around 49.0 and 46.0 T would be expected for ions Fe<sup>3+</sup> and Fe<sup>2.5+</sup> of magnetite at room temperature [20], these values can diminish due to surface anisotropy in particles at nanoscale, where the magnetic moments of ions Fe<sup>3+</sup> and Fe<sup>2.5+</sup> located on the surface are canted with respect to the mean magnetization inside the particles, reducing significantly the magnetic interactions on surface. The doublet with spectral area of 50% is attributed to ions Fe<sup>3+</sup> of superparamagnetic maghemite (SP-Maghemite), which is the main phase expected in the nanocomposite due to the easy oxidation of Fe<sup>2+</sup> to Fe<sup>3+</sup> during the synthesis process.

### 3.1.5 Magnetization measurements

The room temperature magnetization curve of the nanoparticles synthesized is presented in Fig. 5. The sample saturated at a magnetic field of 200 kAm<sup>-1</sup> approximately.

The hysteresis parameters, presented in Table 4, show a low saturation magnetization of 8.48 kAm<sup>-1</sup>, this value being at least 11 times smaller than that of a crystalline and stoichiometric magnetite (92 A m<sup>2</sup> kg<sup>-1</sup>), which can be attributed to the presence of the diamagnetic component of chitosan, which, according to thermogravimetric measurements represents

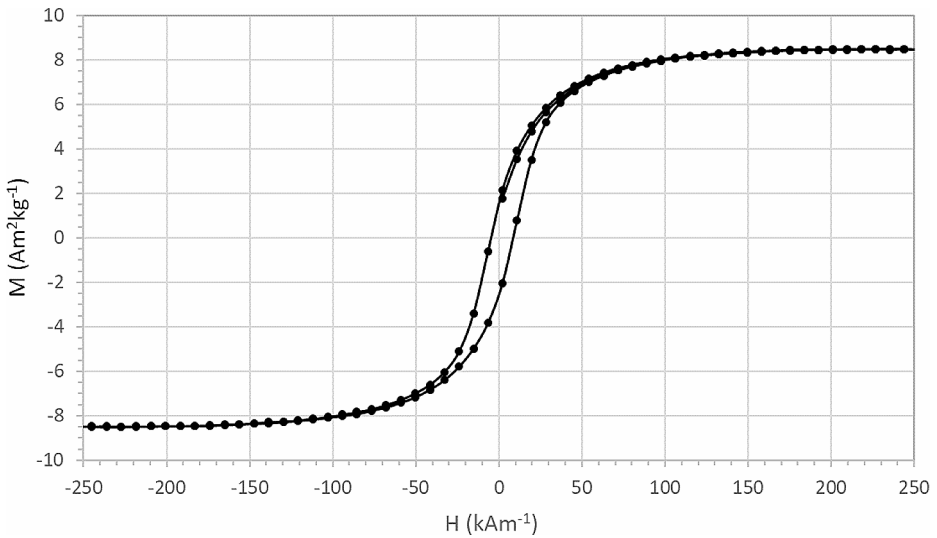


**Fig. 5** Magnetization curve of the nanocomposite synthesized

**Table 4** Hysteresis parameters of the nanocomposites synthesized

$M_s$ ( $A\ m^2\ kg^{-1}$ )	$M_r$ ( $A\ m^2\ kg^{-1}$ )	$H_c$ ( $kA\ m^{-1}$ )
$8.48 \pm 0.01$	$1.90 \pm 0.01$	$8.3 \pm 0.2$

$M_s$  saturation magnetization,  $M_r$  remanent magnetization,  $H_c$  coercive magnetic field

70% of the mass of the sample, as well as possible surface anisotropy effects related to the low dimensions of the nanoparticles.

## 3.2 Application of the aqueous suspensions of nanoparticles in maize seeds

### 3.2.1 Phytotoxicity assay on maize seeds

Phytotoxicity is the ability of some compounds to cause morpho-anatomical, physiological, biochemical and/or genetic damage in plants [21]. The toxicity caused by nanoparticles depends on their concentrations, type, size, chemical structure, reactivity and treated plant species [22], and it is frequently evaluated with the germination rate, biomass accumulation and root length of the germinated seeds, as main measurement parameters [21]. In this study, we evaluated suspensions of nanoparticles with iron contents of 12.5, 25, 50, 75 and 100 ppm (see Fig. 6). After applying these suspensions, the germination percentage of the seeds presented a value greater than 93%, indicating good viability and vigor of the seeds in all treatments [23].

Regarding the behavior of biomass and root length of germinated maize seeds, presented in Fig. 7, the best and simpler model of fit of biomass and root length as a function of the iron content supplied by nanoparticles was quadratic, being the value of the coefficient of determination in both fittings above 88%. A regression analysis of both variables showed that biomass and root length have a statistically significant relationship with the iron content



**Fig. 6** Phytotoxicity assay of aqueous suspensions of iron oxide nanoparticles on maize seeds. From left to right, dilution of the suspension of nanoparticles in deionized water, maize seeds in a Petri dish with filter paper moistened with nanoparticles suspension and maize seeds germinated

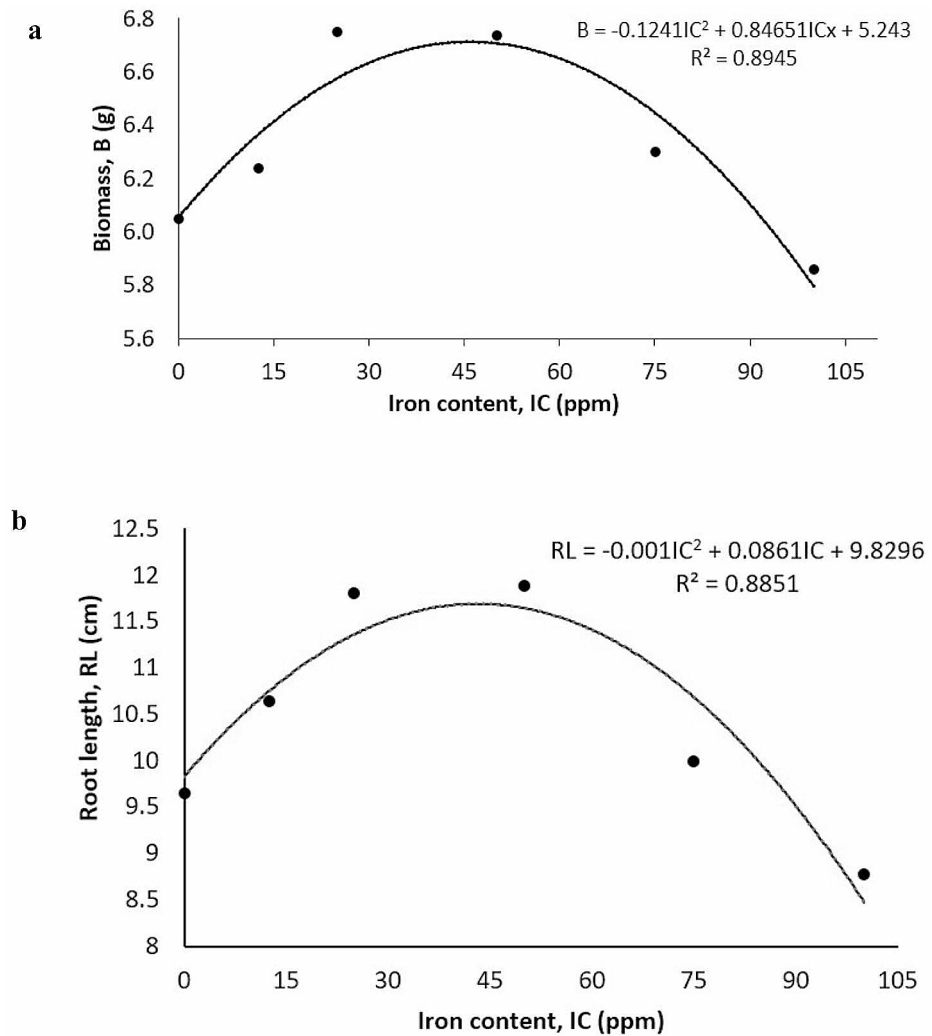


**Fig. 7** Regression analysis of biomass and root length of germinated maize seeds for different iron contents supplied by the suspensions of nanoparticles. **(a)** Evaluation of variable biomass ( $p$ -value: 0.0098), **(b)** Evaluation of variable root length ( $p$ -value: 0.0424). Black dots represent experimental data and black lines represent the fit model

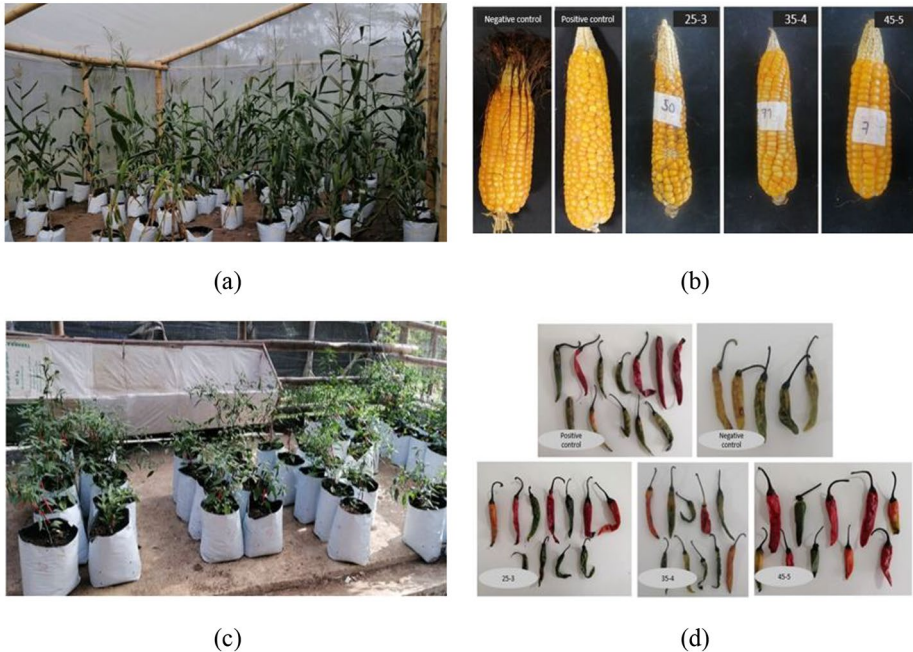


**Fig. 8** Maize and chili pepper plants under greenhouse conditions and their fruits. **(a)** Maize plants in the greenhouse, **(b)** Fruits of maize plants representative of each treatment, **(c)** Chili pepper plants in greenhouse **(d)** Fruits of chili pepper plants representative of each treatment

in the suspensions, with a  $p$ -value less than 0.05 in both cases [24, 25]. According to these results it is possible to conclude that iron contents less than 50 ppm showed a direct relationship with the dependent variables, while suspensions with iron contents higher than 50 ppm showed an inverse relationship. At 100 ppm of iron content, biomass and root length showed lower values than the control, suggesting that suspensions with iron contents of 100 ppm have a phytotoxic effect on maize seeds. In a similar study, Li et al. [26] reported that the application of suspensions of 20 ppm of maghemite nanoparticles on maize seeds, increases the root length, vigor index and germination percentage, nevertheless at iron contents of 50 and 100 ppm root length decreased significantly. In another work [27], it was observed that aqueous suspensions of magnetite nanoparticles covered by citric acid, with contents of nanoparticles of 5, 10, 15 and 20 ppm did not affect the germination rate, the chlorophyll content, and the plant growth of wheat (*Triticum aestivum* L.) under in vitro and hydroponic conditions.

### 3.2.2 Greenhouse assay

Based on results of phytotoxicity, three aqueous suspensions of nanoparticles with iron-phosphorus contents of 25–3, 35–4, 45–5 ppm and tap water as control were chosen to perform greenhouse assays on maize and chili pepper plants, in order to evaluate the effect of these suspensions in the morpho-anatomical and physiological parameters of these plants. On the one hand, the maize plants evaluated grew satisfactorily, with an average

number of 10 dark green leaves per plant, with primary and secondary root formation, and male (panicle) and female (cob) flower development (Fig. 8a). The fruits of all the plants treated with the different treatments were cylindrical in shape, with yellow grains of hard morphology, but none of them had a complete filling of grains (Fig. 8b). On average, in all treatments, the number of rows per cob was 12 and the number of grains was 27, characteristic values of this maize variety according to the technical data sheet developed by the International Center for Tropical Agriculture, CIAT [28]. On the other hand, a total of 65 plants were harvested and evaluated for the cultivation of chili pepper, which had a good rooting process, bifurcation of branches, flowering and fruit development during their phenological cycle (Fig. 8c). In addition, these plants presented oval leaves and dark green color, with fruits of elongated morphology with different ripening stages represented in a certain color, green (unripe fruit), yellow (medium ripe fruit) and red (ripe fruit). According to Fig. 8d, the plants that achieved the highest number of ripe fruits under the test conditions were those treated with suspensions of nanoparticles 45–5 ppm, suggesting that this concentration could be influencing the ripening process of chili pepper fruits.

For quantitative analysis, we measured the following morphological parameters in all harvested plants of both crops: height, stem thickness, dry biomass and fruit weight. According to these results, shown in Fig. 9, none of the morphological and physiological measurements performed on the plants showed a statistically significant difference between the evaluated treatments compared to the control, except for dry biomass in chili pepper, which showed a statistically significant difference between the treatment 35–4 ppm and the control. These results suggest that the suspensions of nanoparticles used in these assays does not harm the growth and development of the plants, under the iron contents and experimental conditions of this evaluation, except for the 35–4 ppm concentration which suggests a negative effect on the dry biomass as it has a lower value than the control.

## 4 Conclusions

We have evaluated the effect of applying aqueous suspensions of magnetite-maghemite nanoparticles functionalized with chitosan and phosphates on yellow maize and chili pepper plants. According to a phytotoxicity test, the germination percentage of maize seeds was optimal for all treatments with suspensions with iron contents ranging from 12.5 to 100 ppm. Nevertheless, germinated maize seeds treated with suspensions with iron contents higher than 50 ppm showed a decreasing trend of biomass and root length compared to those of seeds treated with suspensions with lower iron contents and water. The application of suspensions with iron contents of 100 ppm led to morphological and physiological parameters lower than those obtained with the control, suggesting phytotoxic effects of suspensions with iron contents higher than this one. On the other hand, maize and chili pepper plants treated under greenhouse conditions with suspensions of nanoparticles with iron-phosphorus contents of 25–3, 35–4 and 45–5 ppm did not show adverse effects on germination, plant height, stem thickness, dry biomass and fruit weight. Only the treatment of chili pepper with a suspension 35–4 ppm led to a dry biomass lower than that of the control, suggesting that these iron-phosphorus contents could have a negative effect on the dry weight parameter of this crop. Nevertheless, additional experiments are required to confirm this adverse effect on chili pepper. In general, no significant differences in morphological

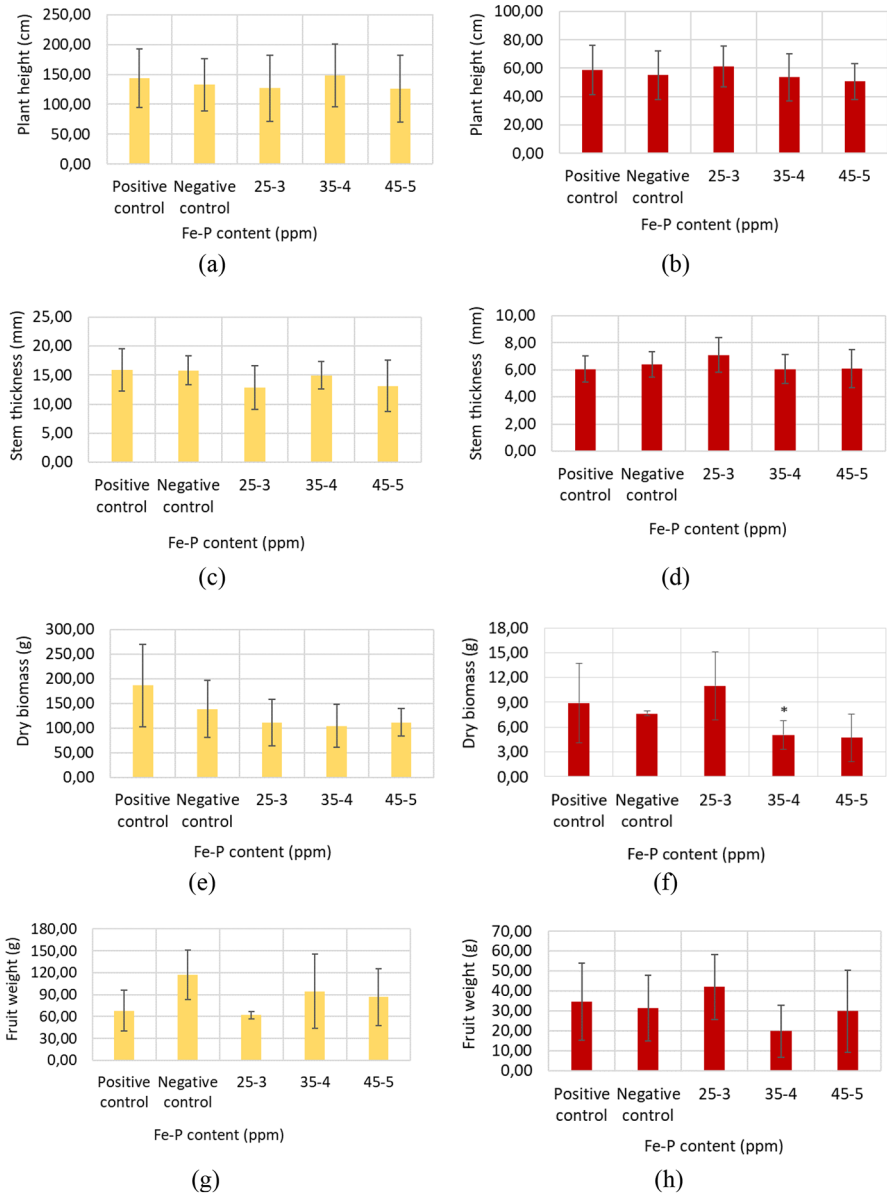


**Fig. 9** Graphs of morpho-anatomical and physiological measurements made on plants grown and developed under greenhouse conditions. **(a)** Plant height of maize ( $p$ -value: 0.741), **(b)** Plant height of chili pepper ( $p$ -value: 0.234), **(c)** Maize stem thickness ( $p$ -value: 0.562), **(d)** Chili pepper stem thickness ( $p$ -value: 0.787), **(e)** Dry biomass of maize ( $p$ -value: 0.072), **(f)** Dry biomass of chili pepper ( $p$ -value: 0.011; Dunnett test: 0.018 between control and 35–4 ppm treatments), **(g)** Fruit weight of maize ( $p$ -value: 0.232), **(h)** Fruit weight of chili pepper ( $p$ -value: 0.242)

and physiological development parameters of seeds and seedlings were observed among all treatments of maize and chili pepper crops. This research provides additional evidence to those reported in the state of the art on the effect of the use of spinel iron oxide nanoparticles stabilized with biocompatible polymers on plants, which may be relevant for research projects aimed at evaluating the impact of nanomaterials in the agricultural sector.

**Supplementary Information** The online version contains supplementary material available at <https://doi.org/10.1007/s10751-024-01843-y>.

**Acknowledgements** The authors of this work thank the “Centro de Laboratorios: CLAB” from EAFIT University for the support given to this research through laboratory equipment services to perform different physical and chemical measurements of the crops.

**Author contributions** A.A Velásquez participated in the design of the experiments, synthesis and characterization of magnetic nanoparticles, analyzes of data, manuscript writing and project management. J.P Urquijo participated in the synthesis and characterization of magnetic nanoparticles and manuscript writing. Y.A. Montoya participated in the design of the experiments, crop monitoring, data acquisition, statistical analyzes of data and manuscript writing. D.M Susunaga participated in crop monitoring, plant’s measurements and statistical analyzes of data. D.F Villanueva participated in the design of the experiments, analysis and monitoring of biological parameters of the plants.

**Funding** Open access funding provided by Colombia Consortium. This research was possible thanks to the funding support given by “Universidad EAFIT” from Medellín, as well as “Ministerio de Ciencia, Tecnología e Innovación- Minciencias” from Colombia, through the project program “Conectando conocimiento 852, 2019”, code Minciencias 70459.

Open Access funding provided by Colombia Consortium

**Data availability** The statistical analysis of data obtained from maize and chili pepper plants, the disinfection protocol of maize and chili pepper seeds, data with the original Mössbauer spectrum, the fitted spectrum and the hyperfine parameters obtained by fitting are included as supplementary material. The remainder tissues of plants were stored in a cool room located in the Biology laboratory of EAFIT University, Medellín headquarters. These tissues are not available in a public herbarium.

## Declarations

**Ethical approval** Not applicable.

**Competing interests** The authors declare no competing interests.

**Open Access** This article is licensed under a Creative Commons Attribution 4.0 International License, which permits use, sharing, adaptation, distribution and reproduction in any medium or format, as long as you give appropriate credit to the original author(s) and the source, provide a link to the Creative Commons licence, and indicate if changes were made. The images or other third party material in this article are included in the article’s Creative Commons licence, unless indicated otherwise in a credit line to the material. If material is not included in the article’s Creative Commons licence and your intended use is not permitted by statutory regulation or exceeds the permitted use, you will need to obtain permission directly from the copyright holder. To view a copy of this licence, visit <http://creativecommons.org/licenses/by/4.0/>.

## References

1. Mangalampalli, B., Naresh, D., Paramjit, G.: *Allium Cepa* Root Tip Assay in Assessment of Toxicity of Magnesium Oxide nanoparticles and Microparticles. *J. Environ. Sci.* **66**, 125–137 (2018). <https://doi.org/10.1016/j.jes.2017.05.012>

2. Roco, M.C.: Broader Societal issues of Nanotechnology. *J. Nanopart. Res.* **5**(3), 181–189 (2003). <https://doi.org/10.1023/A:1025548512438>
3. Carvalho, C.H.T.L.E., Pereira, L.B., Montanha, A.E.S., Corrêa, G.S., Carvalho, C.G., Ganin, H.W.P., Fraceto, A.Y., L.F., and, Yiu, H.H.P.: Localization of Coated Iron Oxide (Fe<sub>3</sub>O<sub>4</sub>) nanoparticles on Tomato seeds and their effects on Growth. *ACS Appl. Biomaterials.* **3**(7), 4109–4117 (2020). <https://doi.org/10.1021/acsabm.0c00216>
4. Yang, Z., Cheng, J., Dou, R., Gao, X., Mao, C., Wang, L.: Assessment of the phytotoxicity of metal oxide nanoparticles on two crop plants, Maize (*Zea Mays* L.) and Rice (*Oryza Sativa* L.). *Int. J. Environ. Res. Public Health.* **12**(12), 15100–15109 (2015). <https://doi.org/10.3390/ijerph121214963>
5. Ruttkay-Nedecky, B., Krystofova, O., Nejdil, L., Adam, V.: Nanoparticles based on essential metals and their phytotoxicity. *J. Nanobiotechnol.* **15**(1), 1–19 (2017). <https://doi.org/10.1186/s12951-017-0268-3>
6. Gogos, A., Knauer, K., Bucheli, T.D.: Nanomaterials in Plant Protection and Fertilization: Current state, Foreseen Applications, and Research priorities. *J. Agr Food Chem.* **60**(39), 9781–9792 (2012). <https://doi.org/10.1021/jf302154y>
7. Sundaria, N., Singh, M., Upreti, P., Chauhan, R., Jaiswal, J.P., Kumar, A.: Seed priming with Iron Oxide nanoparticles triggers Iron Acquisition and Biofortification in Wheat (*Triticum aestivum* L.) grains. *J. Plant. Growth Regul.* **38**, 122–131 (2019). <https://doi.org/10.1007/s00344-018-9818-7>
8. Rui, M., Ma, C., Hao, Y., Guo, J., Rui, Y., Tang, X., Zhao, Q., Fan, X., Zhang, Z., Hou, T., Zhu, S.: Iron Oxide nanoparticles as a potential Iron fertilizer for peanut (*Arachis hypogaea*). *Front. Plant. Sci.* **7**(815), 1–10 (2016). <https://doi.org/10.3389/fpls.2016.00815>
9. Frank, L.A., Onzia, G.R., Morawskib, A.S., Pohlmann, A.R., Guterres, S.S., Contri, R.V.: Chitosan as a coating material for nanoparticles intended for biomedical applications. *React. Funct. Polym.* **147**, 1–14 (2020). <https://doi.org/10.1016/j.reactfunctpolym.2019.104459>
10. Shukla, S., Jadaun, A., Arora, V., Sinha, R.K., Biyani, N., Jain, V.K.: In vitro toxicity assessment of chitosan oligosaccharide coated iron oxide nanoparticles. *Toxicol. Rep.* **2**, 27–39 (2015). <https://doi.org/10.1016/j.toxrep.2014.11.002>
11. Ruihua, H., Bingchao, Y., Sheng, D., Wang, B.: Preparation and characterization of a quaternized chitosan. *J. Mater. Sci.* **47**, 845–851 (2012). <https://doi.org/10.1007/s10853-011-5862-4>
12. Sarvendra, K., Patra, A.K., Datta, S.C., Rosin, K.G., Purakayastha, T.J.: Phytotoxicity of nanoparticles to seed germination of plants. *Int. J. Adv. Res.* **3**(3), 854–865 (2015)
13. Velásquez, A.A., Trujillo, J.M., Morales, A.L., Tobón, J.E., Reyes, L., Gancedo, J.R.: Design and construction of an Autonomous Control System for Mössbauer Spectrometry. *Hyperfine Interact.* **161**, 139–145 (2005). <https://doi.org/10.1007/s10751-005-9176-2>
14. Maqbool, M.A., Beshir, A.R., Khokhar, E.S.: Quality protein maize (QPM): Importance, genetics, timeline of different events, breeding strategies and varietal adoption. *Plant Breed.* **140**(3), 375–399 (2021). <https://doi.org/10.1111/pbr.12923>
15. Azlan, A., Sultana, S., Huei, C.S., Razman, M.R.: Antioxidant, Anti-obesity, Nutritional and other Beneficial effects of different Chili Pepper: A review. *Molecules.* **27**(3), 2–11 (2022). <https://doi.org/10.3390/molecules27030898>
16. Gutiérrez, H., De La Vara, R.: Análisis Y diseño de experimentos, segunda edición. Mc Graw Hill, Mexico (2008)
17. Dong, C.: PowderX: Windows-95-based program for powder X-ray diffraction data processing. *J. Appl. Crystallogr.* **32**, 168–173 (1999). <https://doi.org/10.1107/S0021889899003039>
18. Lutterotti, L., Matthies, S., Wenk, H.R.: MAUD: A friendly Java program for material analysis using diffraction int. *Union Crystallogr. Newsl.* **21**, 14–15 (1999)
19. Vandenberghe, R., De Grave, E., De Bakker, P.M.A.: On the methodology of the analysis of Mössbauer Spectra. *Hyperfine Interact.* **83**, 29–49 (1994)
20. Mössbauer Effect Data Center, Mössbauer Mineral Handbook, 404: (2005)
21. Tripathi, D.K., Shweta, Singh, S., Singh, S., Pandey, R., Singh, V.P., Sharma, N.C., Prasad, S.M., Dubey, N.K., Chauhan, D.K.: An overview on manufactured nanoparticles in plants: Uptake, translocation, accumulation and phytotoxicity. In *Plant Physiology and Biochemistry.* **110**, 2–12 (2017). <https://doi.org/10.1016/j.plaphy.2016.07.030>
22. Feng, Y., Kreslavski, V.D., Shmarev, A.N., Ivanov, A.A., Zharmukhamedov, S.K., Kosobryukhov, A., Yu, M., Allakhverdiev, S.I., Shabala, S.: Effects of Iron Oxide nanoparticles (Fe<sub>3</sub>O<sub>4</sub>) on growth, photosynthesis, antioxidant activity and distribution of Mineral Elements in Wheat (*Triticum aestivum*) plants. *Plants.* **11**(14), 1–15 (2022). <https://doi.org/10.3390/plants11141894>
23. Steil, A.: How to Store Seeds and Test Germination Rates. IOWA State University, Culture and Home Pest News. Available: (2023). <https://hortnews.extension.iastate.edu/how-store-seeds-and-test-germination-rates#:~:text=For%20most%20species%20C%20a%20germination,naturally%20have%20lower%20germination%20rates>

24. Humpage, S.: An introduction to regression analysis. *Sens.* (Peterborough NH). **17**(9), 68–74 (2000). <https://doi.org/10.1002/9781118267912.ch6>
25. Looman, N.: Regression. In *Data analysis in community and landscape ecology* (pp. 29–77). Cambridge University Press. Available: (1967). <https://library.wur.nl/WebQuery/wurpubs/fulltext/249377>
26. Li, J., Hu, J., Ma, C., Wang, Y., Wu, C., Huang, J., Xing, B.: Uptake, translocation and physiological effects of magnetic iron oxide ( $\gamma$ -Fe<sub>2</sub>O<sub>3</sub>) nanoparticles in corn (*Zea mays* L). *Chemosphere*. **159**, 326–334 (2016). <https://doi.org/10.1016/j.chemosphere.2016.05.083>
27. Iannone, M.F., Groppa, M.D., de Sousa, M.E., van Fernández, M.B., Benavides, M.P.: Impact of magnetite iron oxide nanoparticles on wheat (*Triticum aestivum* L.) development: Evaluation of oxidative damage. *Environ. Exp. Bot.* **131**, 77–88 (2016). <https://doi.org/10.1016/j.envexpbot.2016.07.004>
28. CIAT, fenalce: CIMMYT & AgroSalud: Maíz de alta calidad de proteína. (2010)

**Publisher's Note** Springer Nature remains neutral with regard to jurisdictional claims in published maps and institutional affiliations.

## Authors and Affiliations

A. A. Velásquez<sup>1</sup> · J. P. Urquijo<sup>2</sup> · Y. A. Montoya<sup>3</sup> · D. M. Susunaga<sup>3</sup> · D. F. Villanueva-Mejía<sup>3</sup>

---

✉ A. A. Velásquez  
avelas26@cafit.edu.co

<sup>1</sup> Grupo de Electromagnetismo Aplicado, Universidad EAFIT, Medellín A.A. 3300, Colombia

<sup>2</sup> Grupo de Estado Sólido, Universidad de Antioquia, Medellín A.A. 1226, Colombia

<sup>3</sup> Grupo de Ciencias Biológicas y Bioprocesos, Universidad EAFIT, Medellín A.A. 3300, Colombia